Nanoscale

Triplet Photosensitizer-Nanotube Conjugates: Synthesis, Characterization and Photochemistry of Charge Stabilizing, Palladium Porphyrin/Single-Walled Carbon Nanotube Conjugates

Journal:	*Nanoscale*
Manuscript ID	NR-ART-03-2020-002136.R1
Article Type:	Paper
Date Submitted by the Author:	21-Apr-2020
Complete List of Authors:	Arellano Castellanos, Luis; Universidad de Castilla-La Mancha Facultad de Ciencias Ambientales y Bioquimica, Organic Chemistry Gobeze, Habtom; University of North Texas, Chemistry Gómez-Escalonilla, Maria; University of Castilla-La Mancha, Organic Chemistry Fierro, Jose Luis; d. Instituto de Catálisis y Petroleoquímica, CSIC, Cantoblanco, 28049, Madrid, Spain D'Souza, Francis; University of North Texas, Chemistry Langa, Fernando; University de Castilla-la Mancha, Institute for Nanoscience and Molecular Materials

ARTICLE

Triplet Photosensitizer-Nanotube Conjugates: Synthesis, Characterization and Photochemistry of Charge Stabilizing, Palladium Porphyrin/Single-Walled Carbon Nanotube Conjugates

Received 00th January 20xx,
Accepted 00th January 20xx

DOI: 10.1039/x0xx00000x

Luis M. Arellano,[a] Habtom B. Gobeze,[b] María J. Gómez-Escalonilla,[a] José Luis G. Fierro,[c] Francis D'Souza[b,*] and Fernando Langa[a,*]

The ability of a triplet photosensitizer to generate long-lived charge separated states, in contrast to traditionally used singlet photosensitizers, in covalently functionalized single-walled carbon nanotube hybrids has been investigated. Enriched single-walled carbon nanotubes with two diameters, namely (6,5) and (7,6), were covalently modified to carry a charge-stabilizing triplet photosensitizer derived from a palladium porphyrin. The nanohybrids were fully characterized and the presence of intramolecular interactions between the porphyrin and nanotubes was established from various spectroscopic, imaging, electrochemical and thermochemical studies. Photoluminescence of palladium porphyrin was found to be quantitatively quenched in the presence of covalently appended SWCNTs and this quenching is due to excited state charge separation has been established by femtosecond transient absorption studies. Owing to the presence of the triplet photosensitizer, the charge separated states lasted over 3 ns, i.e., much longer than those reported earlier for singlet photosensitizer-derived nanotube hybrids. The nanohybrids also exhibited efficient photocatalytic behavior in experiments involving electron pooling of one-electron reduced methyl viologen in the presence of a sacrificial electron donor. Higher yields of photoproducts were achieved from the present donor-acceptor nanohybrids when compared with those of singlet photosensitizer-derived nanohybrids, more so for (6.5) nanotube derived hybrids compared to (7,6) nanotube derived hybrids. The present findings highlight the importance of triplet photosensitizer derived nanohybrids in artificial photosynthesis of charge separation and photocatalytic applicatons.

This work is dedicated to the memory of Prof. Jose Luis García-Fierro, who passed away recently.

Introduction

Extending the lifetime of charge-separated states in donor-acceptor conjugates has been a major challenge in artificial photosynthesis of solar energy harvesting.[1-17] The formation of sufficiently long-lived charge separated states is key in developing the next generation of photocatalysts for light-to-electricity and light-to-fuel conversion.[18,19] In natural photosynthesis[9-15, 18-22] the charge-separation is stabilized by sequential electron or hole transfer involving multiple electron acceptors or donors, and such a phenomenon has been successfully accomplished in synthetic model compounds.[23-31] In donor-acceptor dyads, charge separation from the excited singlet state of the donor or acceptor must be rapid to outperform the process of intersystem crossing (ISC),[32-34] and since the charge separation originates from the singlet excited state, the lifetime of the charge separated states in such donor-acceptor conjugates is low, thus making it difficult to engage them in photocatalytic applications. An alternative approach to produce long-lived charge separated states is to design donor-acceptor conjugates with high-energy triplet photosensitizers. Since the lifetime of the triplet-excited states is longer, the rate of electron transfer could be slower and this could allow the donor and acceptor to be further apart. Furthermore, since the charge separated species is generated initially with a triplet spin multiplicity, this also delays the recombination to the singlet ground state.[35] However, building donor-acceptor conjugates in which the charge separation exclusively occurs from the triplet-excited state without interference from the singlet-excited state has been challenging. Recently, our group made some progress in addressing this issue by synthesizing dyads in which palladium(II)porphyrin (PdP) or platinum(II)porphyrin (PtP) were used as photosensitizers. The heavy metals in these porphyrins promoted rapid ISC to produce high energy excited triplet states (1.78–1.89 eV). When such porphyrins were covalently linked to the well-known electron acceptor fullerene, C_{60}, it was possible to produce the much desired long-lived charge separated states.[36-38] Additionally, this approach has

[a] Universidad de Castilla-La Mancha, Instituto de Nanociencia, Nanotecnología y Materiales Moleculares (INAMOL), 45071-Toledo, Spain. E-mail: Fernando.Langa@uclm.es
[b] Chemistry and Materials Science and Engineering, University of North Texas, 76203-5017 Denton, TX, USA. E-mail: Francis.D'Souza@UNT.edu
[c] Instituto de Catálisis y Petroleoquímica, CSIC, Cantoblanco, 28049, Madrid, Spain. E-mail: jlgfierro@icp.csic.es
† Footnotes relating to the title and/or authors should appear here.
Electronic Supplementary Information (ESI) available: [Experimental and synthetic procedures, along with Figs. S1-S18 and Tables S1-S4]. See DOI: 10.1039/x0xx00000x

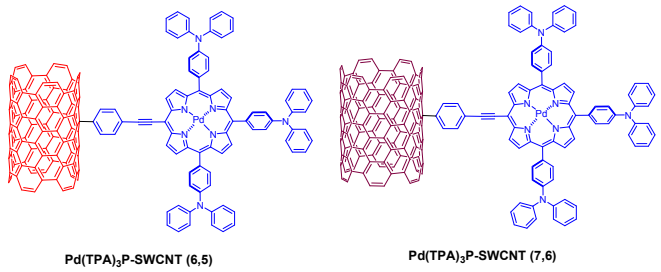

Fig. 1. Structure of the tris(triphenylamino)porphyrinato palladium(II), $Pd(TPA)_3P$ linked to SWCNT(6,5) and SWCNT(7,6) donor-acceptor hybrids investigated in the present study.

allowed the donor and acceptor to be placed at relatively larger distances while requiring less driving force.[36-38]

In donor-acceptor conjugates derived from single-walled carbon nanotubes, charge separation occurs from the singlet-excited state of the photosensitizer or the excitonic state of the nanotubes. However, both charge separation and charge recombination occur within couple of ps, thus limiting their usage in energy harvesting applications.[15,39-53] In the present study, by realizing the significance of triplet photosensitizers in stabilizing the charge separated states, we have employed a charge stabilizing triplet photosensitizer, namely tris(triphenylamino)porphyrin palladium(II), $Pd(TPA)_3P$[36-37], linked covalently to single-walled carbon nanotubes of different sizes (Fig. 1). The triphenylamino entities are known to stabilize the charge-separated states.[53-54] These nanohybrids were fully characterized and femtosecond transient absorption spectroscopic studies demonstrated the formation of relatively long-lived charge separated states. Additionally, these donor-acceptor conjugates were engaged as photocatalysts in electron pooling experiments to demonstrate their superior photocatalytic performance.

Experimental

Chemicals and materials

All reactions were carried out under argon using oven-dried glassware. All chemicals were reagent-grade, purchased from commercial sources, and used as received, unless otherwise specified. The (6,5) and (7,6) enriched nanotubes, produced by CoMoCAT,® South West Nano Technologies Inc. (www.swentnano.com), and sold by Sigma Aldrich Co. The (6,5)-SWCNTs were 0.7-0.9 nm in diameter, average length of 1 micron, mostly semiconducting, and of ~ 95% purity, while the (7,6)- SWCNTs were 0.7-1.1 nm in diameter, average length of 1 micron, mostly semiconducting and of ~ 95% purity.

Dry triethylamine (NEt_3) was prepared according to the literature procedure.[55] The palladium (II) 5 ethynyltrimethylsilane-[10,15,20-tri-(N,N-diphenylaniline)-] porphinato **4** was prepared according to literature procedures (ESI).[56-58]

Synthesis of iodophenyl enriched SWCNTs (SWCNTs-I (6,5) and (7,6))

Pristine (6,5) or (7,6) enriched SWCNT (40 mg, 3.33 mmol) was dispersed in *N*-methyl-2-pyrrolidone (NMP) (80 mL) by ultrasonication for 10 min. Nitrogen was bubbled through the suspension for 2 min and 4-iodoaniline (1.46 g, 6.66 mmol) and isoamyl nitrite (1.07 mL, 8 mmol) were added. The reaction mixture was stirred for 12 h at 70 °C under an argon atmosphere. The reaction mixture was cooled to room temperature and filtered through a 0.1 µm pore size OMNIPORE membrane and the black solid was collected and washed with different solvents (NMP), methanol and dichloromethane (DCM) several times until the filtrate was colourless. Finally, the black solid material was dried overnight in a vacuum oven at 55 °C to obtain the carbon-based materials SWCNTs-I (6,5) and SWCNTs-I (7,6) as black solids.

Synthesis of hybrids 1-2:

To a solution of **4** (40 mg, 0.03 mmol) in DCM (8 mL), 1 M tetra-*n*-butylammonium fluoride (TBAF) in THF (1.25 mmol) was introduced. The mixture was maintained under an argon atmosphere and stirred at room temperature for 5 h. The reaction was quenched with water and extracted with DCM (3 × 25 mL). The combined organic layers were dried over anhydrous Na_2SO_4 and the solvent was removed under reduced pressure to afford the unprotected porphyrin **3** quantitatively. Functionalized iodophenyl SWCNTs-I (6,5) or (7,6) (30 mg) and NMP (45 mL) were placed in a microwave glass vessel, sonicated for 15 min at room temperature and degassed; then **3** (40 mg, 0.03 mmol), tris(dibenzylideneacetone) dipalladium(0) ($Pd_2(dba)_3$) (3 mg, 3.27×10^{-3} mmol), triphenylarsine ($AsPh_3$) (21 mg, 0.07 mmol) and degassed NEt_3 (15 mL) were added and the glass vessel was stoppered with a septum and placed in the microwave reactor. Microwave irradiation (50 W) was applied for 1 h at 150 °C. The resulting paste was filtered through a 0.1 µm pore size OMNIPORE membrane to remove the solvent and the unreacted reagents. The product was washed thoroughly with NMP, methanol, acetone and DCM until a persistently colourless filtrate was obtained. The black material was dried under vacuum at 55 °C to afford functionalized SWCNTs **1** and **2**.

Results and discussions

Synthesis of covalently linked tris(triphenylamino)porphyrinato palladium(II)-SWCNT hybrids

The synthetic strategy followed to obtain the new modified carbon nanotubes **1** and **2** is described in Scheme 1. Palladium (II) 5-trimethylsilylethynyl-10,15,20-tri-[*p*-(*N*,*N* diphenylamino) phenyl]porphinate **4** was prepared by a previously reported procedure (see Experimental in ESI);[57] subsequent treatment with TBAF gave compound **3**, which bears a terminal alkyne subunit. Furthermore, the modification

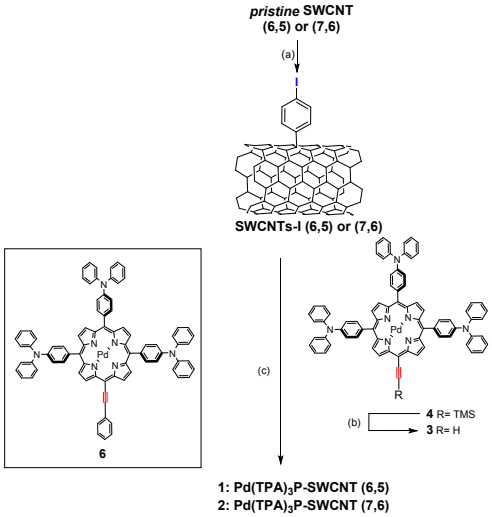

Scheme 1. Synthetic approach for the preparation of nanoconjugates **1** and **2**. *Reagents and conditions:* (a) 4-iodoaniline, isoamyl nitrite, NMP, 70 °C, 12 h; (b) TBAF, 0 °C to rt, 5 h; (c) **3**, $Pd_2(dba)_3$, $AsPh_3$, NEt_3, NMP, MWI, 50 W, 1 hour, 150 °C. Reference porphyrin compound **6** structure are included.

of *pristine* SWCNT(6,5) and (7,6) sidewalls was performed by adding 4-iodobenzenediazonium salt,[58] generated *in situ* from 4-iodoaniline and isoamyl nitrite, to afford SWCNTs-I. Finally, unprotected porphyrin building block **3** was linked onto the corresponding *p*-iodophenyl functionalized SWCNTs through copper-free Sonogashira cross-coupling reaction[41-45] under microwave irradiation (MWI)[59] to afford functionalized carbon nanotubes **1** and **2**. The properties of both nanohybrids were compared to those of the reference porphyrin derivative **6** (see Scheme 1 and further details in Electronic Supporting Information, Figs. S1-S8).

In order to secure detailed information on the structural, electronic and chemical properties, nanoconjugates **1** and **2** were fully characterized by a range of analytical techniques, which included thermogravimetric analysis (TGA), Fourier transform infrared spectroscopy (FTIR), Raman, X-ray photoelectron spectroscopy (XPS), atomic force microscopy (AFM), electrochemistry and steady-state and time-resolved spectroscopic techniques.

The first evidence for successful carbon nanotube functionalization was obtained by TGA. The thermal profiles of functionalized SWCNTs (**1** and **2**) are represented in Fig. S1 together with those of their SWCNT (6,5) and (7,6) precursors and reference porphyrin **6**. At 700 °C, the thermograms revealed a loss of weight of about 11.3% for *pristine* SWCNT (6,5), 21.9% for SWCNTs-I (6,5) and 33.8% for **1** (Fig. S9, left). The loss of weight observed for *pristine* SWCNT (6,5), between 200 °C and 700 °C may be due to the destruction of the residual amorphous carbon still present in the nanotubes and to the decarboxylation of the oxidized species. The corrected weight losses due to the functional groups on carbon nanotubes were then estimated to be 10.6% and 22.5% for SWCNTs-I (6,5) and hybrid **1** , respectively (weight loss difference of SWCNTs-I (6,5) – *pristine* SWCNT (6,5) and **1** – *pristine* SWCNT (6,5)). The number of iodophenyl functional groups in SWCNTs-I (6,5) was then estimated as 1 per 152 carbon atoms. With the same calculation, we estimated the amount of functional groups as 1 per 414 carbon atoms for $Pd(TPA)_3P$-SWCNT(6,5). On the other hand, at 700 °C porphyrin **6** shows a weight loss of 48%. Since the weight loss corresponding to the coupled porphyrin is about 11.9% in hybrid **1** (**1** – SWCNTs-I (6,5)), the amount of grafting porphyrin in $Pd(TPA)_3P$-SWCNT(6,5) may correspond to a real ratio of *ca.* 25% (11.9%/48%). Then, the number of functional groups in this case can be estimated to one porphyrin per 104 carbon atoms. The differences observed in these calculations are corroborated by XPS data (see Tables S1-S2 in ESI) confirming that the extent of the Sonogashira coupling reaction was limited, as observed in previous works.[44] TGA data for hybrid **2** are detailed in Fig. S9 (right) in ESI.

Raman spectroscopy also provided conclusive support for the successful covalent functionalization of SWCNTs. The degree of functionalization was calculated based on the intensity ratio of the D-band to the G-band (D/G ratio). This intensity is associated with the introduction of defects into the carbon nanostructure surface due to the change in the hybridation of sp^2 carbon atoms to sp^3; in order to obtain information about the homogeneity of the introduced defects, statistical Raman spectroscopy (SRS)[60-61] was applied by analysing the I_D/I_G ratio of the materials using a 785 nm excitation laser (>700 single point spectra; scanning Raman map

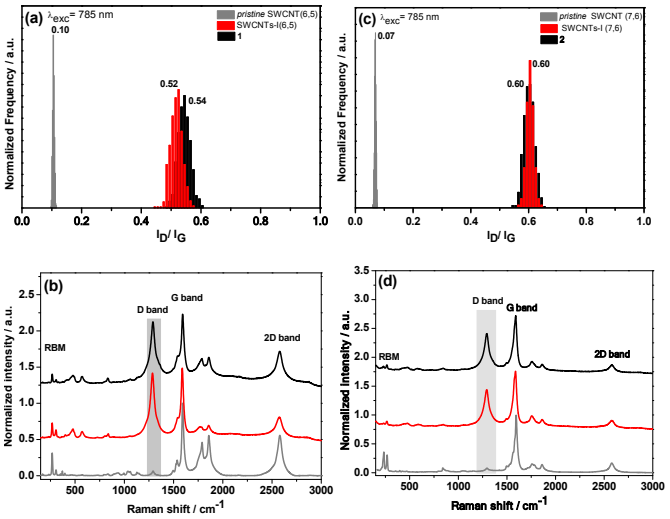

Fig.2 Statistical Raman spectroscopy (>700 single point spectra each) of *pristine* SWCNTs (—), SWCNTs-I (—) and nanoconjugates **1** and **2** (—) (a,c): statistical distribution of I_D/I_G values at 785 nm laser excitation wavelength; (b,d): average spectra at 785 nm laser excitation wavelength.

at least 15 x 15 μm^2). As can be seen in Figs. 2(b) and (d), *pristine* SWCNT materials exhibit two narrow peaks, D-band at ~1285 cm^{-1} and G-band at ~1590 cm^{-1}. After the first functionalization with an aryl moiety (SWCNT-I), an increase in the intensity of the D-band was observed and, consequently, the I_D/I_G ratio also increased due to the introduction of sp^3 defects on the CNT surface. However, in the second modification with the incorporation of porphyrin **3**, new peaks derived from the porphyrin moieties could not be observed, probably due to the emission background of porphyrin, which normally prevents the acquisition of a Raman spectrum with distinct features.[62] The

statistical analysis of the I_D/I_G ratio of functionalized materials (see Figs. 3(a) and (c)), compared with *pristine* enriched SWCNTs, revealed the successful covalent modification of the CNT sidewall without a contribution from non-functionalized or *pristine* SWCNTs. It is worth to mention that the I_D/I_G ratio remained nearly constant for **1** and **2** nanoconjugates compared with their corresponding SWCNTs-I derivatives, suggesting that the grafting of the palladium porphyrin occurs on the iodophenyl moieties rather than on the SWCNT sidewalls. These results are consistent with XPS data (see below).

Raman spectroscopy was also used to verify n-doping or p-doping effects in CNTs.[63] Nanoconjugates **1** and **2** showed a downshift by ~ 5 cm^{-1} in the G-band (Fig. S10) when compared with *pristine* nanotube sample and this was consistent with previous findings for the covalent modification of SWCNTs with porphyrins,[42] thus suggesting the n-doping effect of the porphyrin molecule on semiconducting nanotubes. Similar effects can also be observed in the 2D band[64] (Fig. S11) in both nanohybrids in comparison to the starting carbon nanotube.

X-ray photoelectron spectroscopy (XPS) was employed to measure changes in the elemental composition of the SWCNTs as a result of the cross-coupling reactions. The binding energies of the main components (C1s, O1s, N1s, Pd3d and I3d) are summarized in Table S1. Treatment of enriched SWCNTs with the diazonium salt led to the clear appearance of the I3d doublet. Both of the samples exhibited the typical I3d doublet, the main components of which appear at *ca.* 620.1 eV (I3d5/2) and *ca.* 631.5 eV (I3d3/2).[65] After Sonogashira coupling, a decrease in iodine content relative to *pristine* SWCNTs was observed, as one would expect, and the nitrogen and palladium contents increased - a finding that is consistent with the introduction of palladium porphyrin **3** onto the CNT surface.[66] Quantitative data were also obtained from XPS measurements (see Table S2 in ESI). A small amount of iodine remained after Sonogashira coupling reaction on the surface of the two chiral substrates and this indicates that porphyrin anchorage is not complete, as observed in previous works.[44,67] Moreover, the N/Pd ratios of 6.5 and 6.3 for nanoconjugates **1** and **2**, respectively, indicate that the palladium porphyrin **3** moiety was incorporated to the functionalized SWCNT surface in a molecular form.

The FTIR spectra of the two nanoconjugates (**1** and **2**) showed absorption peaks around 1480 to 1580 cm^{-1} and these are assigned to porphyrin macrocycle (C=C and C=N stretching vibrations) (Fig. S12). These results are in agreement with XPS and TGA data and corroborate the successful covalent functionalization of the carbon nanotubes.

AFM images revealed the existence of individual nanotubes with an average height of 0.93 nm and 1.07 nm for *pristine* SWCNT(6,5) and SWCNT(7,6) , respectively (see Fig. S13). After functionalization (Fig. 3), an increase in the height of ~ 2 nm was observed in both hybrids and this change is consistent with the distance calculated for the skeletal structure of the palladium porphyrin addend by means of theoretical calculations (Fig. S14 in ESI).

The UV-vis-NIR spectra of *functionalized* enriched CNTs were recorded for comparison with reference porphyrin **6** and *pristine* chiral CNTs using (NMP) as solvent (Fig. 4 and Fig. S15). The spectra of nanohybrids **1** and **2** displayed the key features of the constituent porphyrin, with a small red-shift (~5 cm^{-1} for **1** and ~2 cm^{-1} for **2**) in the absorption maxima (Soret band) corresponding to the porphyrin chromophore (438 nm), when

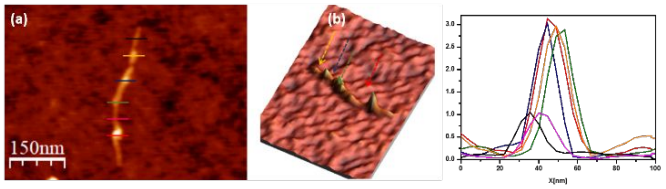

Fig. 3 AFM topographic (a) and 3-dimensional (b) images of hybrid 1 isolated on a SiO_2 surface with height profiles taken along the nanotube marked in (b), showing a height increment of ca. 2 nm for the indicated zones. The colour code is shown in the images.

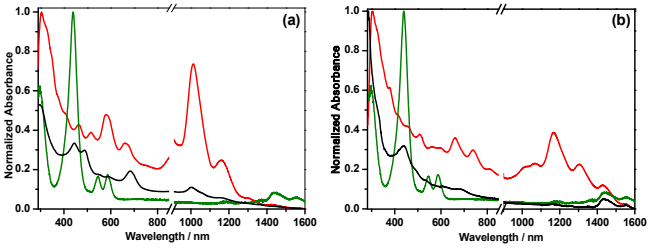

Fig. 4 Steady-state absorption spectra of: (a) **1** (—), **6** (—) and *pristine* SWCNT (6,5) (—) and (b) **2** (—), **6** (—) and *pristine* SWCNT (7,6) (—), registered in NMP.

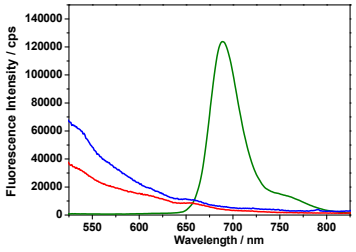

Fig. 5 Steady state luminescence spectra of reference porphyrin **6** (—) compared to the nanoconjugates **1** (—) and **2** (—) in DMF (λ_{ex} = 440 nm).

compared with that of reference **6**, which suggests the existence of electronic interactions between CNTs and porphyrin in the ground state.[44] Similar results were observed in the polar solvent *N,N*-dimethylformamide (DMF) (Figs. S16).

In order to find evidence for the excited-state interactions between the porphyrin moiety and SWCNTs, luminescence spectra of the hybrids **1** and **2** and porphyrin **6** were measured in DMF (Fig. 5). An emission band was observed at 690 nm upon excitation at the Soret band (440 nm) of **6** in DMF but in hybrids the emission was quenched quantitatively (Fig. 5), which suggests the occurrence of excited-state events such as electron or energy transfer between the porphyrin and the carbon nanotubes.[44]

The 3D photoluminescence excitation (PLE) maps provide more information about covalent functionalization on the sidewall of CNT, since the introduction of sp^3 defects into sp^2 carbon networks can create a new optically allowed defect state.[68,69]

This change modifies the E_{11} and E_{11}^{-} excitonic transition and the PL is red-shifted and can be over 10 times brighter. The corresponding 3D photoluminescence plots for *pristine* enriched SWCNT (6,5) and derivatives are shown in Fig. 6. A red shift in the photoluminescence from 981 to 1128 nm was detected in SWCNTs-I (6,5) (see Table S3 in ESI). However, the incorporation of porphyrin **3** through C-C coupling to afford hybrid **1** barely changed the PL map because the previously created defects were still present and new defects were not formed (see Table S3). Similar results were found for the (7,6) derivative (Fig. S17).These results provide further evidence for the covalent bonding on the sidewall of CNTs.

The redox properties of hybrids **1** and **2** were determined by Osteryoung Square Wave Voltammetry (OSWV) in benzonitrile

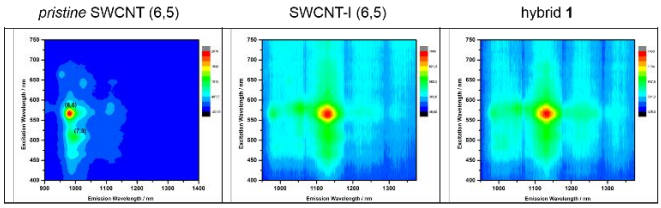

Fig. 6 Excitation–emission PL maps of *pristine* SWCNT (6,5), SWCNTs-I (6,5) and hybrid **1**. All spectra in D_2O with 2% SDBS as surfactant and acquired at room temperature.

(PhCN) and the results were compared with those of model **6**. For the sake of comparison, electrochemical measurements were also carried out with *free base* **5** (see Experimental Section in ESI). The electrochemical data for nanohybrids **1–2** and porphyrins **5** and **6** are collected in Table S4 (see further details in Fig. S18). Free base porphyrin **5** displays three oxidations located at +0.49, +0.71 and +0.88 V. For metallated porphyrin **6**, the oxidations were located at +0.61 and +0.87 V; in this case, the first oxidation involved both palladium porphyrin[70] and the peripheral TPA entities while the second oxidation was assigned to the porphyrin macrocycle. The first oxidation potentials of **1** and **2** are shifted to more positive values by 40 mV and 30 mV, respectively, relative to **6** (see Table S4), which suggests the occurrence of intramolecular interactions in the ground state between the two electroactive moieties, namely, Pd-porphyrin and carbon nanotube.[44]

The redox chemistry of SWCNTs was reported by Tanaka and co-workers using near-infrared photoluminescence spectroelectrochemistry.[72] For SWCNTs (6,5) and (7,6), oxidation potentials of 0.64 and 0.50 V and reduction potentials of -0.43 and -0.41 V *vs.* Ag/AgCl, respectively, were arrived. From the emission peak position of **6**, an excitation energy of 1.80 eV was estimated. Using the redox potentials and excitation energy of the photosensitizer, free-energy charges for charge separation, ΔG_{cs} was estimated according to Rehm-Weller approach,[66] by neglecting solvation energy term. Such calculations resulted in ΔG_{cs} values of -0.76 and -0.78 eV for $Pd(TPA)_3P^{\cdot+}$-$SWCNT(6,5)^{\cdot-}$ and $Pd(TPA)_3P^{\cdot+}$-$SWCNT(7,6)^{\cdot-}$ formation, respectively, indicating thermodynamic feasibility of excited state charge separation in these nanohybrids.

Femtosecond transient absorption studies

Femtosecond transient absorption studies were performed in an effort to witness excited state charge transfer in these nanoconjugates. The fs-TA spectra of triplet sensitizer $Pd(TPA)_3P$ is shown in Fig. 7a. Fast intersystem crossing was observed and this lead to long-lived $^3Pd(TPA)_3P^*$ in less than 30 ps. The $^3Pd(TPA)_3P^*$ was characterized by peaks at 498, 631, 858 and 1228 nm and negative signals at 550 and 588 nm related to ground state bleaching. The one-electron oxidized product of $Pd(TPA)_3P$ was also characterized in a spectroelectrochemical study, as shown in Fig. 7b. The $Pd(TPA)_3P^{\cdot+}$ was characterized by new peaks at 426 and 530 nm. The appearance of such signals provides evidence of excited state charge transfer upon photoexcitation in the nanoconjugates, wherein the porphyrin serves as a photosensitizer-electron donor. The fs-TA spectra of SWCNT(6,5) in the visible and near-IR regions at an excitation wavelength of 585 nm are shown in Figs. 7c and d. The broad absorbance of the nanotubes allows them to be excited using most of the visible light. Optical excitonic peaks with depleted peak maxima at 678 and 1010 nm were observed for the SWCNT(6,5) sample dispersed in DMF. Recovery of these peaks was rapid with a new peak appearing at 1272 nm, which was earlier ascribed to triplet state of nanotubes.[73] The $Pd(TPA)_3P$ SWCNT(6,5) dispersion was excited at the same wavelength and this excited mainly $Pd(TPA)_3P$ and to some extent the SWCNT(6,5) entity (Figs. 7e and f). Noticeable changes were observed for the conjugate when compared to the individual components.

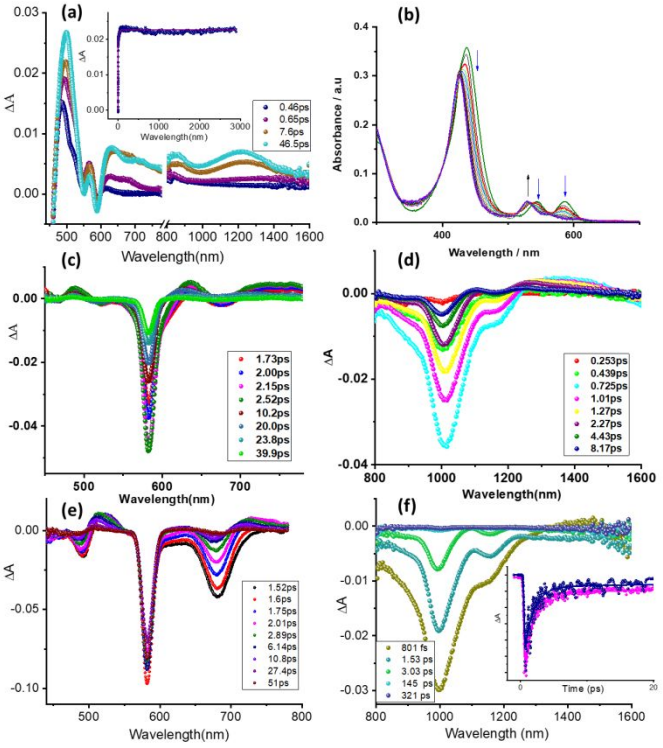

Fig. 7 Femtosecond transient absorption spectra at the indicated delay times of (a) $Pd(TPA)_3P$ at an excitation wavelength of 440 nm (inset – time profile of the 498 nm peak showing triplet population), (b) spectral changes during first oxidation of $Pd(TPA)_3P$, (c and d) SWCNT (6,5) at an excitation wavelength of 585 nm and (e and f) $Pd(TPA)_3P$ SWCNT(6,5) at an excitation wavelength of 585 nm.

All spectra were recorded in deaerated DMF. Figure 7f inset shows the time profile of the 1010 nm peak of $Pd(TPA)_3P$ SWCNT (6,5) (blue) and (SWCNT (6,5) (magenta).

First, the excitonic peak was much more intense and was slightly blue-shifted. For example, the near-IR peak located at 1010 nm in the pristine sample appeared at 998 nm. The higher intensity could be attributed to better solubility of the conjugate due to the appended organics or it could be as a result of rapid excitation transfer. More importantly, a positive signal around 530 nm, which was not observed for either of the starting materials, whose peak position matched that of $Pd(TPA)_3P^{\cdot+}$ provided direct proof for excited state charge transfer. It may be pointed out here that nanotubes do not display new peaks corresponding to nanotube anions,[73] except for diminished intensity of the of the ΔE_{11}^{S} and ΔE_{22}^{S} peaks. Hence, transient peak of $Pd(TPA)_3P^{\cdot+}$ is mainly used to provide evidence of charge separation. A depleted peak at 492 nm was observed and this suggests that the $^3Pd(TPA)_3P^*$ is indeed involved in the charge separation process. In the near-IR region, relaxation of the excitonic peak was much more rapid (see Fig. 8f inset for time profiles at early time scales), but a peak was not present in the 1272 nm region where the triplet of nanotubes was observed,[73] thus suggesting that charge separated state and the directly excited nanotubes relax to the ground state in the nanohybrids. The 530 nm peak intensity lasted over 3 ns, the maximum delay time of our transient set up, suggesting existence of long-lived charge separated species, which is much longer than that reported earlier for singlet sensitizer derived, *i.e.*, porphyrin or phthalocyanine appended nanotube conjugates.[43,44]

We proceed to focus our attention on SWCNT (7,6)-derived conjugates. SWCNT (7,6) dispersions in DMF showed major excitonic peaks at 690 and 1170 nm (see Fig. 8a) and the majority of the intensity was recovered in about 110 ps. Interestingly, the spectroscopic features were sufficiently different for $Pd(TPA)_3P$-SWCNT(7,6) dispersions in DMF. As expected, a broad peak at around 530 nm, which is characteristic of $Pd(TPA)_3P^{\cdot+}$, was observed and this peak also lasted beyond 3 ns. The excitonic peak of SWCNT (7,6) at 690 and in the near-IR region of 1170 nm were much broader (Figs. 8c and d) with a small red shift as a consequence of covalent functionalization. The time profile of the 1170 nm peak within the first 20 ps is shown in Fig. 8b and faster recovery of $Pd(TPA)_3P$-SWCNT(7,6) was observed when compared to *pristine* SWCNT(7,6). Importantly, transient spectroscopic studies allowed us to establish the charge separation process and witness relatively long-lived charge separated states (over 3 ns) owing to the presence of triplet photosensitizer. This situation is in contrast to the singlet photosensitizers, where majority of the charge separated state persisted for only few ps.[43,44]

The formation of relatively long-lived charge separated states prompted us to perform photocatalytic electron pooling studies involving a sacrificial electron donor, 1-benzyl-1,4-dihydronicotinamide (BNAH) and an electron acceptor methyl viologen (MV^{2+}).[68,69] In the process, continuous irradiation (a Xenon lamp with a 400 nm filter was used) of a mixture $Pd(TPA)_3P$-SWCNT nanoconjugates in the presence of MV^{2+} and BNAH lead to accumulation of $MV^{\cdot+}$ with a characteristic peak at 610 nm. Energetically, direct electron transfer from BNAH to MV^{2+} is an uphill process;[74-75] however, charge separated state species could make this process a thermodynamically feasible. As shown in Fig. 9, increased addition of BNAH increased the intensity of $MV^{\cdot+}$ for both $Pd(TPA)_3P$-SWCNT(6,5) and $Pd(TPA)_3P$ -SWCNT(7,6) nanohybrids.

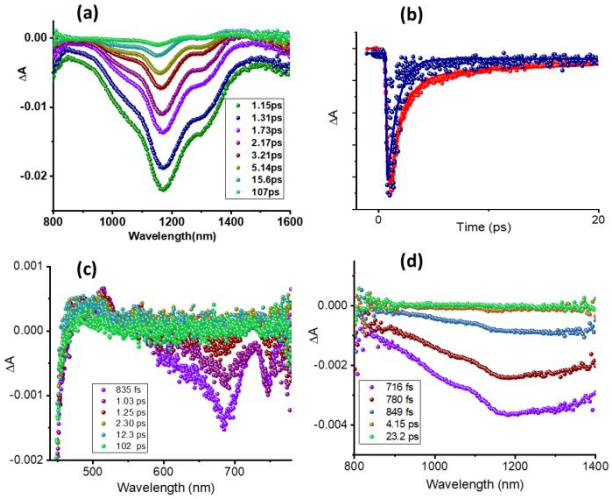

Fig. 8. fs-TA spectra at the indicated delay times of (a) SWCNT (7,6) at the excitation wavelength of 662 nm, (c and d) $Pd(TPA)_3P$-SWCNT (7,6) at the excitation wavelength of 440 nm exciting primarily $Pd(TPA)_3P$. (b) The time profile of the 1170 nm peak of SWCNT (7,6) (red) and $Pd(TPA)_3P$-SWCNT (7,6) (blue). All spectra were recorded in deaerated DMF.

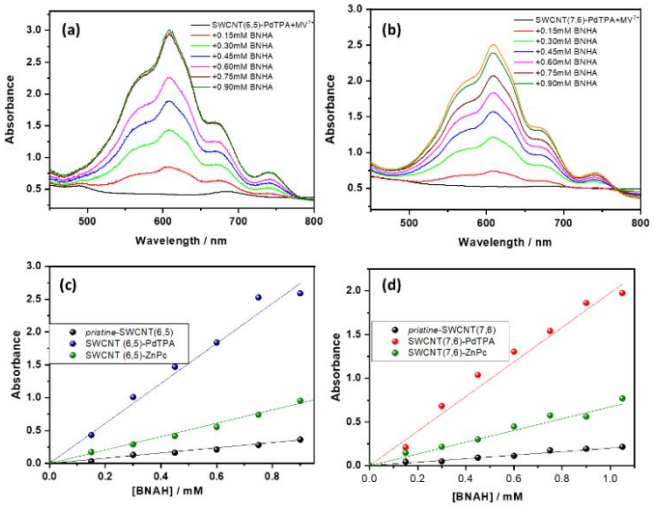

Fig. 9 Electron pooling experiments on (a) $Pd(TPA)_3P$-SWCNT(6,5) and (b) $Pd(TPA)_3P$-SWCNT(7,6) nanohybrids in DMF containing 0.5 mM MV^{2+} upon addition of increasing amounts of BNAH. (b) Extent of $MV^{\cdot+}$ formation with respect to pristine nanotube and ZnPc derived SWCNT nanohybrids is also shown.

Control experiments performed on ZnPc-SWCNT (6,5) and ZnPc-SWCNT (7,6) nanohybrids[44] with singlet photosensitizers and *pristine* SWCNTs revealed relatively lesser accumulation of $MV^{\cdot+}$ and this suggests the importance of the triplet sensitizer derived

donor-acceptor nanohybrids for improved photocatalytic applications.

Conclusions

Diameter-sorted single-walled carbon nanotubes were covalently modified to incorporate charge-stabilizing triplet photosensitizers derived from palladium porphyrin. Various spectroscopic, imaging, electrochemical and thermochemical techniques were used to characterize the nanohybrids and to visualize interactions between the photosensitizer with the carbon nanotube π-system. The presence of SWCNTs quenched the photoluminescence of the palladium porphyrin almost quantitatively, and the free-energy calculations supported excited state charge separation. The quenching mechanism indeed due to excited state charge separation was established from femtosecond transient absorption studies in which it was possible to spectroscopically characterize the charge-separated states. The charge separated states lasted over 3 ns, i.e., much longer than those reported earlier for singlet photosensitizer-derived nanohybrids. The nanohybrids were further subjected to photocatalytic investigation involving electron pooling studies. Higher yields of photoproduct, viz., one electron reduced methyl viologen, were achieved from the current donor-acceptor nanohybrids when compared those with singlet photosensitizer derived nanohybrids. Between the two types of nanotubes used in the present study, performance of (6,5) enriched nanotube derived hybrid was slightly better than that of (7,6) enriched nanotube derived hybrid.

Conflicts of interest

There are no conflicts to declare.

Acknowledgements

This research was financially supported by the Spanish Ministry of Economy and Competitiveness of Spain (CTQ2016-79189-R), Junta de Comunidades de Castilla-La Mancha (SBPLY/17/180501/000254) and FEDER funds and US-National Science Foundation (Grant number 1401188 to FD). L. M. A. thanks MINECO for a doctoral FPI grant.

References

1 D. Gust, T. A. Moore and A. L. Moore, *Acc. Chem. Res.*, 2009, **42**, 1890-1898.
2 M. R. Wasielewski, *Acc. Chem. Res.*, 2009, **42**, 1910-1921.
3 M. E. El-Khouly, O. Ito, P. M. Smith and F. D'Souza, *J. Photochem. Photobiol. , C,* 2004, **5**, 79-104.
4 L. Sánchez, N. Martín and D. M. Guldi, *Angew. Chem., Int. Ed.,* 2005, **44**, 5374-5382.
5 S. Fukuzumi, *Phys. Chem. Chem. Phys.,* 2008, **10**, 2283-2297.
6 S. Fukuzumi, K. Ohkubo, F. D'Souza and J. L. Sessler, *Chem. Commun.,* 2012, **48**, 9801-9815.
7 O. Ito and F. D'Souza, *Molecules,* 2012, **17**, 5816-5835.
8 G. Bottari, G. de la Torre, D. M. Guldi and T. Torres, *Chem. Rev.* 2010, **110**, 6768-6816.
9 D. M. Guldi, G. M. A. Rahman, V. Sgobba and C. Ehli, *Chem. Soc. Rev.,* 2006, **35**, 471-487.
10 H. Imahori, T. Umeyama, K. Kurotobi and Y. Takano, *Chem. Commun,.* 2012, **48**, 4032-4045.
11 F. D'Souza and O. Ito, *Chem. Soc. Rev.,* 2012, **41**, 86-96.
12 S. Fukuzumi and T. Kojima, *J. Mater. Chem.,* 2008, **18**, 1427-1439.
13 *Organic Nanomaterials*, ed, T. Torres and G. Bottari, Wiley, Hoboken, NJ, 2013.
14 M. E. El-Khouly, S. Fukuzumi and F. D'Souza, *ChemPhysChem,* 2014, **15**, 30-47.
15 M. Barrejon, L. M. Arellano, F. D'Souza and F. Langa, *Nanoscale*, 2019, **11**, 14978-14992.
16 T. Umeyama , J. Baek , Y. Sato, K. Suenaga, F. Abou-Chahine, N. V. Tkachenko, H. Lemmetyinen and H. Imahori, *Nat. Commun.*, 2015, **6**, 7732.
17 T. Umeyama and H. Imahori, *Nanoscale Horiz.,* 2018,**3**, 352-366.
18 T. Umeyama and H. Imahori, *Energy Environ. Sci.,* 2008, **1**, 120-133.
19 T. Hasobe, *Phys. Chem. Chem. Phys.,* 2010, **12**, 44-57.
20 *The Photosynthetic Reaction Center*, ed. J. Deisenhofer and J. R. Norris, Academic Press, New York, 1993.
21 *Molecular Mechanism of Photosynthesis*, ed. R. E. Blankenship, Blackwell Science, Oxford, 2002.
22 *The Porphyrin Handbook*, ed. K. M. Kadish, K. M. Smith and Guilard R., Academic Press, San Diego, CA, 2000.
23 J. L. Delgado, P. Bouit, S. Filippone, M. A. Herranz and N. Martin, *Chem. Commun.,* 2010, **46**, 4853-4865.
24 S. Fukuzumi, K. Ohkubo, H. Imahori, J. Shao, Z. Ou, G. Zheng, Y. Chen, R. K. Pandey, M. Fujitsuka, O. Ito and K. M. Kadish, *J. Am. Chem. Soc.,* 2001, **123**, 10676-10683.
25 H. Imahori, Y. Sekiguchi, Y. Kashiwagi, T. Sato, Y. Araki, O. Ito, H. Yamada and S. Fukuzumi, *Chem. - Eur. J.,* 2004, **10**, 3184-3196.
26 D. M. Guldi, H. Imahori, K. Tamaki, Y. Kashiwagi, H. Yamada, Y. Sakata and S. Fukuzumi, *J. Phys. Chem. A,* 2004, **108**, 541-548.
27 H. Imahori, D. M. Guldi, K. Tamaki, Y. Yoshida, C. Luo, Y. Sakata and S. Fukuzumi, *J. Am. Chem. Soc.,* 2001, **123**, 6617-6628.
28 V. Balzani, G. Bergamini and P. Ceroni, *Coord. Chem. Rev.,* 2008, **252**, 2456-2469.
29 G. N. Lim, E. Maligaspe, M. E. Zandler and F. D'Souza, *Chem. - Eur. J.,* 2014, **20**, 17089-17099.
30 C. B. KC, G. N. Lim and F. D'Souza, *Nanoscale,* 2015, **7**, 6813-6826.
31 P. K. Poddutoori, G. N. Lim, A. S. D. Sandanayaka, P. A. Karr, O. Ito, F. D'Souza, M. Pilkington and A. van der Est, *Nanoscale,* 2015, **7**, 12151-12165.
32 *Electron Transfer in Chemistry*, Vols. 1-4, ed. Balzani, V. Wiley-VCH, Weinheim, 2001-2002.
33 *Photoinduced Electron Transfer*; Vols. A-D, M. A. Fox, M. Chanon, Elsevier, Amsterdam, 1988.
34 Topics in Current Chemistry: *Photoinduced Electron Transfer*, Vol 156-157, ed. J. Mattay, Springer-Verlag, Berlin, 1990.
35 T. Higashino, T. Yamada, M. Yamamoto, A. Furube, N. V. Tkachenko, T. Miura, Y. Kobori, R. Jono, K. Yamashita and H. Imahori, *Angew. Chem., Int. Ed.,* 2016, **55**, 629-633.
36 C. O. Obondi, G. N. Lim, B. Churchill, P. K. Poddutoori, A. van der Est, and F. D'Souza, *Nanoscale*, 2016, **8**, 8333-8344.
37 D. R. Subedi, H. B. Gobeze, Y. E. Kandrashkin, P. K.

Poddutoori, A. van der Est and F. D'Souza, *Chem. Commun*. 2020, in press. DOI: 10.1039/d0cc02007a

38 P. K. Poddutoori, Y. E. Kandrashkin, C. O. Obondi, F. D'Souza and A. van der Est, *Phys. Chem. Chem. Phys.* 2018, **20**, 28223-28231.

39 G. Bottari, G. de la Torre and T. Torres, *Acc. Chem. Res.*, 2015, **48**, 900-910.

40 K. H. Le Ho, L. Rivier, B. Jousselme, P. Jégou, A. Filoramo and S. Campidelli, *Chem. Commun.*, 2010, **46**, 8731-8733.

41 M. Barrejón, S. Pla, I. Berlanga, M. J. Gómez-Escalonilla, L. Martín-Gomis, J. L. García-Fierro, M. Zhang, M. Yudasaka, S. Iijima, H. B. Gobeze, F. D'Souza, Á. Sastre-Santos and F. Langa, *J. Mater. Chem. C*, 2015, **3**, 4960-4969.

42 M. Barrejón, H. B. Gobeze, M. J. Gómez-Escalonilla, J. L. García-Fierro, M. Zhang, M. Yudasaka, S. Iijima, F. D'Souza and F. Langa, *Nanoscale*, 2016, **8**, 14716-14724.

43 L. M. Arellano, L. Martín-Gomis, H. B. Gobeze, D. Molina, C. Hermosa, M. J. Gómez-Escalonilla, J. L. García-Fierro, Á. Sastre-Santos, F. D'Souza and F. Langa, *Nanoscale*, 2018, **10**, 5205-5213.

44 L. M. Arellano, M. Barrejón, H. B. Gobeze, M. J. Gómez-Escalonilla, J. L. G. Fierro, F. D'Souza and F. Langa, *Nanoscale*, 2017, **9**, 7551-7558.

45 L. M. Arellano, L. Martín-Gomis, H. B. Gobeze, M. Barrejón, D. Molina, M. J. Gómez-Escalonilla, J. L. García-Fierro, M. Zhang, M. Yudasaka, S. Iijima, F. D'Souza, F. Langa and Á. Sastre-Santos, *J. Mater. Chem. C*, 2015, **3**, 10215-10224.

46 F. G. Brunetti, C. Romero-Nieto, J. Lopez-Andarias, C. Atienza, J. L. Lopez, D. M. Guldi, *Angew. Chem. Int. Ed*. 2013, **52**, 2180-2184.

47 C. Romero-Nieto, R. Garcia, M. A. Herranz, C. Ehli, M. Ruppert, A. Hirsch and D. M. Guldi, *J. Am. Chem. Soc*., 2012, **134**, 9183-9192.

48 T. Umeyama, T. Tomokazu, K. Noriyasu, F. Kawashima, S. Seki, Y. Matoni, Y. Nakao, T. Shishido, N. Tesuya, M. Niki, K. Hirao, H. Lehtivouri, N. V. Tkachenko, H. Lemmetyinen, and H. Imahori, *Angew. Chem. Int. Ed*. 2011, **50**, 4615-4619.

49 D. M. Guldi, G. M. A. Rahman, N. Jux, D. Balbinot, U. Hartnagel, N. Tagmatarchis, M. Prato, *J. Am. Chem. Soc*. 2005, **127**, 9830-9838.

50 D. M. Guldi, G. M. A. Rahman, N. Jux, N. Tagmatarchis, M. Prato, *Angew. Chem. Int. Ed*. 2004, **43**, 4426-5530.

51 K. Rao, G. Venkata, S. J. George, *Chem. Eur. J*. 2012, **18**, 14286-14291.

52 D. M. Guldi, G. M. A. Rahman, V. Sgobba, N. A. Kotov, D. Bonifazi, M. Prato, *J. Am. Chem. Soc*. 2006, **128**, 2315-2323.

53 E. Fazio, K.A. Winterfeld, A. López-Pérez, T. Torres, D.M. Guldi and G. de la Torre, *Nanoscale,* 2018, **10**, 22400-22408.

54 F. D'Souza, S. Gadde, D.M.S. Islam, C. A. Wijesinghe, A. L. Schumacher, M. E. Zandler, Y. Araki and O. Ito. *J. Phys. Chem. A* 2007, **111**, 8552-8560.

55 D. D. Perrin, W. L. F. Armarego and D. R. Perrin, *Purification of Laboratory Chemicals*, vol 1, 2nd ed. Pergamon, *1980*.

56 A. Aljarilla, J. N. Clifford, L. Pellejà, A. Moncho, S. Arrechea, P. de la Cruz, F. Langa and E. Palomares, *J. Mater. Chem. A*, 2013, **1**, 13640–13647.

57 S. Fu Xunjin Zhu, G. Zhou, W.-Y. Wong, C. Ye, W.-K. Wong and Z. Li, *Eur. J. Inorg. Chem*., 2007, 2004–2013.

58 T. Palacin, H. L. Khanh, B. Jousselme, P. Jegou, A. Filoramo, C. Ehli, D. M. Guldi and S. Campidelli, *J. Am. Chem. Soc*., 2009, **42**, 15394-15402.

59 P. de la Cruz and F. Langa, *Comb. Chem. Hight. Scr.,* 2007, **10**, 766-782.

60 J. M. Englert, P. Vecera, K. C. Knirsch, R. A. Schäfer, F. Hauke and A. Hirsch, *ACS Nano*, 2013, **7**, 5472-5482.

61 F. Hof, S. Bosch, J. M. Englert, F. Hauke and A. Hirsch, *Angew. Chem. Int. Ed.*, 2012, **51**, 11727-11730.

62 D. Dasler, R. A. Schafer, M. B. Minameyer, J. F. Hitzenberger, F. Hauke, T. Drewello and A. Hirsch, *J. Am. Chem. Soc.,* 2017, **139**, 11760−11765.

63 J.-L. Xu, R.-X. Dai, Y. Xin, Y.-L. Sun, X. Li, Y.-X. Yu, L. Xiang, D. Xie, S.-D. Wang and T.-L. Ren, *Sci. Rep*., 2017, **7**, 6751.

64 K. Dirian, S.Backes, C. Backes, V. Strauss, F.Rodler, F. Hauke, A. Hirsch and D. M. Guldi, *Chem. Sci.*, 2015, **6**, 6886-6895.

65 Q. Zhao, Y. Lu, Z. Zhu, Z. Tao, J. Chen, *Nano Lett.*, 2015, **15**, 5982-5987.

66 R. Xing, H. Yang, S. Li, J. Yang, X. Zhao, Q. Wang, S. Liu and X. Liu, *J. Solid State Electrochem.,* 2017, **21**, 1219-1228.

67 M. E. Lipinska, S. L. H. Rebelo, M. F. R. Pereira, J. A. N. F. Gomes, C. Freire and J. L. Figueiredo, *Carbon*, 2012, **50**, 3280-3294.

68 Y. Piao, B. Meany, L. R. Powell, N. Valley, H. Kwon, G. C. Schatz and Y. Wang, *Nat. Chem.,* 2013, **5**, 840-845.

69 S. Ghosh, S. M. Bachilo, R. A. Simonette, K. M. Beckingham and R. B. Weisman, *Science*, 2010, **330**, 1656-1659.

70 C. Matlachowski and M. Schwalbe, *Dalton Trans*., 2013, **42**, 3490-3505.

71 Y. Tanaka, Y. Hirana, Y. Niidome, K. Kato, S. Saito and N. Nakashima, *Angew. Chem. Int. Ed*. 2009, **48**, 7655-7659.

72 D. Rehm and A. Weller*, Isr. J. Chem*. 1970, **7**, 259-271.

73 J. Park, P. Deria, M. J. Therien, *J. Am. Chem. Soc*. 2011, **133**, 17156-17159.

74 S. Fukuzumi, H. Imahori, K. Ohkubo, H. Yamada, M. Fujitsuka, O. Ito and D. M. Guldi, *J. Phys. Chem. A,* 2002, **106**, 1903-1908.

75 S. K. Das, C. B. KC and F. D'Souza, *Fullerenes, Nanotubes and Carbon Nanostructures*, 2014, **22**, 128-137.

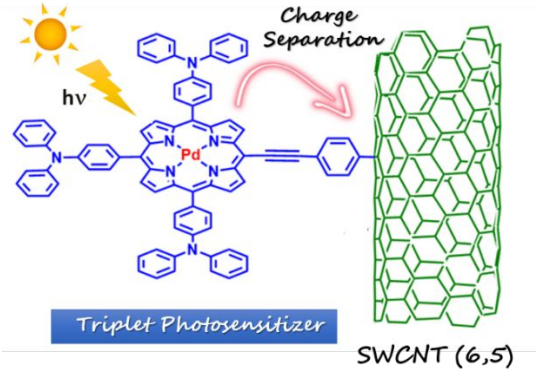

Chirality enriched SWCNTs covalently modified with a charge-stabilizing triplet photosensitizer, palladium porphyrin, have been newly prepared and photoinduced charge separation and photocatalytic properties are reported.